Anal. Bioanal. Electrochem., Vol. 12, No. 1, 2020, 63-80

Analytical & Bioanalytical Electrochemistry

2020 by CEE
www.abechem.com

Full Paper

Electrochemical Behavior of Steels Hastelloy C2000 and SAF 2205 Heat Treated and Inhibition Effect of SO_4^{2-} Against their Corrosion in 1 M H_3PO_4

Afaf Amri,[1,2,*] Mohamed Essahli,[3] Moncef Lamsalmi,[3] Abdelilah Chtaini,[4] Abderrafia Hafid,[4] Amina Ibnlfassi[1] and El Madani Saad[2]

[1]Laboratory of Environmental Sciences and Development, University Hassan 1st, Faculty of Sciences and Technogies, Settat, Morocco
[2]Laboratory of Physical Chemistry of Process and Materials, University Hassan 1st, Faculty of Sciences and Technogies, Settat, Morocco
[3]Laboratory of Applied Chemistry and Environment, University Hassan 1st, Faculty of Sciences and Technogies, Settat, Morocco
[4]Laboratory of Molecular Electrochemistry and Inorganic Materials, University Sultan Moulay Slimane, Faculty of Sciences and Technogies, Béni Mellal, Morocco

*Corresponding Author, Tel.: +212623649237
E-Mail: afaf.amri1@gmail.com

Received: 23 October 2019 / Received in revised form: 17 December 2019 /
Accepted: 19 December 2019 / Published online: 31 January 2020

Abstract- This work continues to focus on evaluating the electrochemical behavior of the steels Hastelloy C2000 and SAF 2205, after heat treatment in 700 °C and 900 °C in 1 M phosphoric acid. In addition, it reports on the effect of sulfate as a corrosion inhibitor of the two steels by using two electrochemical methods Tafel polarization and Electrochemical Impedance Spectroscopy (EIS). The electrochemical characterization of the two steels showed that the corrosion resistance decrease with the elevation of temperature from 700 °C to 900 °C in 1 M H_3PO_4. This decrease is about 76.21% for SAF 2205 and 19.37% for Hastelloy C2000. From these results, SAF 2205 is less resistant to corrosion than Hastelloy C2000 after heat treatment in acid environment. The comparison of the behavior of the two steels in the presence of sulfate showed that the corrosion current intensity of SAF 2205 is higher than that of the Hastelloy C2000. However, the separate analysis of each steel showed, an inhibitory efficiency of 99.99% with the addition of 0.1 g/l of SO_4^{2-} for Hastelloy C2000 and about 91.06% for 0.2 g/l of SO_4^{2-} for SAF 2205 as optimums concentrations.

Keywords- Hastelloy C2000, SAF 2205, heat treatment, corrosion inhibitor, sulfate

---

1. INTRODUCTION

Nowadays, the thorough knowledge of the phenomena affecting the behavior of materials used in the industrial field is an increasing necessity for several sectors: nuclear, aeronautics, petroleum, marine, etc. [1]. Several processes involve the presence of acids as major chemicals products in their production processes. However, the presence of these solutions may constitute an aggressive environment for several materials [2]. Therefore, the choice of these materials, offering excellent corrosion resistance and excellent mechanical properties, have a great importance for the industrial process to extend the life of the equipment and keep the performance at the oxidation.

The use of stainless steel in several areas is due to its many characteristics of mechanical strength and corrosion resistance. However, some steels may be sensitive to a particular form of corrosion such as pitting corrosion [3]. Hence, the importance of the detection of this type of corrosion, which will prevent industrial risks in several areas: economic, safety and environmental.

During the production of phosphoric and sulfuric acid, stainless steels constitute an important part of the building materials of the various installations (agitators, pumps, tanks, pipes) [4,5]. However, the presence of certain impurities such as fluorides and chlorides can cause a dramatic drop in their corrosion resistance, especially when combined with other thermal and mechanical stresses [6,7]. In this context a several studies, have been carried out, on several types of stainless steel to better understand and control the electrochemical behavior of each one in contact with the various aggressive environments such as the more corrosive acid conditions with higher chloride concentrations. These studies have shown that the super austenitic steels, such as X1NiCrMoCu25-20-5, are resistant to these conditions. While for installations requiring operation at high temperatures, austenitic stainless steels with high chromium and molybdenum content are preferred selections for these operating conditions. These alloys include the X1NiCrMoCu32-28-7, NiCr21Mo, NiCr30FeMo, NiCr35FeMo, and NiMo16Cr15W [8,9].

A comparative study in a phosphoric acid, in the presence and the absence of chloride ions, between X1CrNiMoN20-18-6 and NiMo16Cr15W showed that these alloys have the same corrosion resistance [10]. Escrivà-Cerdán [11,12] revealed that the stability of the film formed on the X1NiCrMoCu32-28-7 steel decreased with the increase in the concentration of phosphoric acid polluted by sulfate.

Several studies have also been interested in the effect of SO_4^{2-} ions on the corrosion handling of several types of steel. Among these studies, there is the work of L.J. Yang and al. [13], which found that SO_4^{2-} ions have an inhibitory effect on pitting corrosion. Another study by Y.L. Chou, and al [14], who investigated the combination of SO_4^{2-} and Cl^- ions, showed that when the ratio $[SO_4^{2-}]/[Cl^-]$ is greater than 0,5 the SO_4^{2-} have an inhibitory effect on pitting corrosion.

While for Z.P. Zhu and colleagues [15], they found that SO_4^{2-} could induce pitting corrosion of carbon steel. S.H. Xiong and his collaborators [16] also confirmed that SO_4^{2-} accelerates pitting corrosion of the wall tubes boiler water.

For our study, we choose two types of stainless steels: austenitic of NiCr23Mo16Al and austéno-ferritic of X2CrNiMoN22-5-3 which have become increasingly present in several fields, particularly in the chemical, petrochemical, marine and paper industries [17,18]. The objective of this work is to study the electrochemical behavior of the two steels: NiCr20Mo16Al (Hastelloy C2000) and X2CrNiMoN 22-5-3(SAF 2205) after undergoing heat treatment at two temperatures: 700 °C and 900 °C in a phosphoric acid and also to study the influence of SO_4^{2-} ions on the behavior of the both stainless steels.

2. MATERIALS AND METHODS

In this study, we used two types of stainless steel of different structure: austenitic Hastelloy C2000 and the austeno-ferritic SAF 2205 provided by Haynes International Inc. Small samples of dimensions (18 mm×16 mm×3 mm) are used. These samples were heat treated at two temperatures of 700 °C and 900 °C. The holding time is set at 3 h for each treatment temperature followed by rapid quenching with water. The chemicals compositions of Hastelloy C2000 and SAF 2205, which were the subject of our electrochemical study, are given in Tables 1 and 2 [19].

Table 1. Chemical composition of Hastelloy C2000 in percentage

Ni[a]	Cr	Mo	Cu	Fe	Co	Al	Mn	C	P	Si	Sulfides
59	20-24	15-17	1.3-1.9	3*	2*	0.5*	0.05*	0.01*	0.025*	0.08*	0.01*

*: Maximum percentage; a: balance

Table 2. Chemical composition of SAF 2205 in percentage

C	Si	Mn	Ni	Mo	Cr	P	S	Cu	N
0.030	0.360	1.770	5.700	2.258	22.050	0.018	0.015	0.200	0.140

Electrochemical impedance and polarization spectroscopy analyzes were performed in a three electrodes cell: the working electrode which constitutes the sample to be analyzed with a contact surface of 1 cm^2 (WE); the Ag/AgCl electrode as a reference electrode (RE) and a platinum plate was used as an electrode (PE). These electrodes are connected to a potentiostat, VOLTALAB (PGSTAT 100 model, Eco Chimie B.V., Utrecht, the Low Countries) which controlled by VoltaMaster 4 software. For data processing, it is done by using the software OriginLab.

The potentiodynamic polarization was achieved by scanning the potential at a speed of 100 mV/s ranging from -1000 to 1000 mV. The electrochemical impedance spectroscopy (EIS) curves are performed in a frequency range between 100 kHz and 10 Hz.

In this study, we worked with two electrolytes: an electrolytic consisting of phosphoric acid with a concentration of 1 M, prepared from a commercial solution of high purity (85%). For the second part, which concerns the monitoring of the variation of the current density (i_{corr}) according to the addition of SO_4^{2-}, we have prepared solutions of concentrations varying between 0.1 g/l to 0.7 g/l by dissolving Na_2SO_4 (purity of 98%).

3. RESULTS AND DISCUSSIONS

3.1. Electrochemical behavior of Hastelloy C2000 and SAF 2205 in phosphoric acid

3.1.1. Potentiodynamic Polarization

In order to examine and compare the electrochemical behavior after thermal treatment of Hastelloy C2000 and SAF 2205 in a phosphoric acid at 25 °C, the polarization curves of Tafel for each steel are plotted (Figure 1).

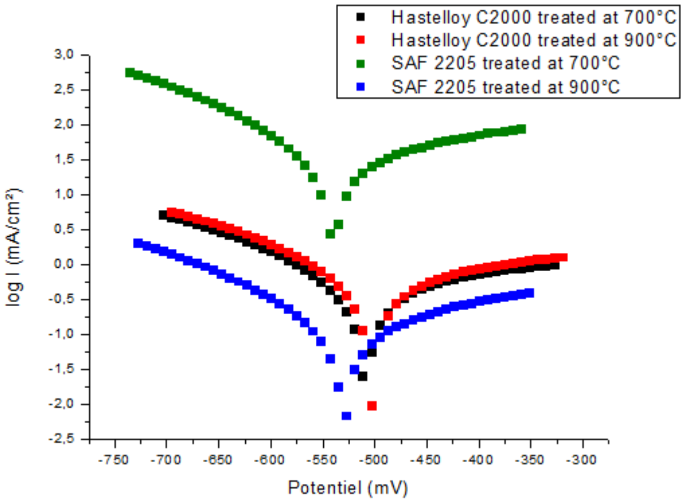

Fig. 1. Tafel polarization curves of Hastelloy C2000 and SAF 2205 after heat treatment at 700 °C and 900 °C in 1 M H_3PO_4 at 100 mV/s

The corrosion parameters, including corrosion potential (E_{corr}), corrosion current density (i_{corr}) and polarization resistance (R_p) from Tafel curves, are summarized in Table 3.

Table 3. Electrochemical parameters characterizing Hastelloy C2000 and SAF 2205 in H_3PO_4 after heat treatment at 700 °C and 900 °C

Steels	**Temperature**	**E_{corr}**	**R_p**	**i_{corr}**
	°C	**mV *vs.* Ag/AgCl**	**Ω.cm²**	**µA/cm²**
Hastelloy C2000	700	-510.00	109.44	310.10
	900	-504.80	88.24	371.00
SAF 2205	700	-541.10	1380.00	21.06
	900	-531.10	328.35	84772.00

We note from these results that the corrosion current intensity of SAF 2205, treated at 900 °C, is higher compared to, Hastelloy C2000 treated at the same temperature. This rate of increase is around 19,63% for Hastelloy C2000. While for the polarization resistance, it decreases with the increase of the temperature of the treatment of the same steel. This result explained with a higher rate for SAF 2205, which is 76,21%, compared to Hastelloy C2000, which represents a decrease of 19,37%. This decrease usually causes a thinning for passive film formed on the electrode, which makes them more porous and less protective [20].

For stainless steel, the composition of the passive film is directly related to the original composition of the steel. Alloy elements such as Cr, Mo and Ni play an important role in the composition and the structure of passive protective film [21,22].

A study, which was carried out on several types of steel, with different molybdenum content, demonstrated that the super austenitic stainless steel X1CrNiMoCuN20-18-6 containing 6% molybdenum was found to be significantly more resistant than X2CrNiMo17-12-2 and X1NiCrMoCu25-20-5; it has relatively the same corrosion resistance as NiMo16Cr15W steel in phosphoric acid in the absence and the presence of chloride ions [10]. This is consistent with the results previously found for our alloys, which have a different percentage of molybdenum in their chemical composition.

Several studies have shown [23,24] that, in phosphoric acid and in the case of stainless steels containing a high Fe content (the case of stainless steel SAF 2205), there is a precipitation of iron phosphates, which are characterized by low solubility. This form of the precipitation occurred in the outer layer of the film according to equations 1 and 2 [24]:

$$6\ H_3PO_4 + 3\ Fe \rightarrow 3\ Fe(H_2PO_4)_2 + 3H_2 \qquad (1)$$

$$3\ Fe(H_2PO_4)_2 \rightarrow Fe_3(PO_4)_2 + 4H_3PO_4 \qquad (2)$$

Based on the literature [25], it was noted that in these phosphoric acid solutions, the outer layer consists of soluble compounds such as $Fe(H_2PO_4)_2$ and other insoluble compounds such as $FeHPO_4$ and $Fe_3(PO_4)_2$. However, the presence of the $Fe(H_2PO_4)_2$ leads to the formation of an outer layer porous film of the passive film.

Huabing Li et al. also showed [24] that, the high levels of the Nickel and the Chrome in phosphoric acid solution lead to the formation of chromium oxide (Cr_2O_3) and nickel oxide (NiO), which usually occur in the inner layer of the film, while forming a compact layer to increase corrosion resistance of the alloy. This explains the variation in the corrosion current intensity between the two steels, in the phosphoric acid, which showed that the corrosion resistance of the SAF 2205 is more affected than that of the Hastelloy C2000, because it corresponds to a difference of 84750,94 $\mu A/cm^2$, comparing to Hastelloy C2000, which has a difference of 60,9 $\mu A/cm^2$. The same behavior was observed for the nickel-based super alloy NiCr23Mo16Al in the same electrolytic solution [26].

Another study on the austenitic stainless steel X1NiCrMoCu25-20-5, also showed that the corrosion resistance of this type of steel is higher in phosphoric acid, compared to other types and this is directly related to the characteristics of the passive film formed on their surface [27,28].

3.1.2. Electrochemical Impedance Spectroscopy

Electrochemical Impedance Spectroscopy (EIS) is used to evaluate the dielectric properties of the passive layer of the both steels and it helps explain the electrochemical process that develops through the latter.

The representation of the electrochemical impedance data Z(ω) by the Nyquist diagram is obtained by plotting on an orthonormal plane the opposite of the imaginary part of the impedance $-Z_i$ as a function of the real part Z_r for the different frequencies.

In the equation 3, the expression for Z(ω) is composed of a real and an imaginary part. If the real part is plotted on the X-axis and the imaginary part is plotted on the Y-axis of a chart, we get a "Nyquist Plot" (Figure 2). Notice that in this plot the Y-axis is negative and that each point on the Nyquist Plot is the impedance at one frequency. Figure 2 has been annotated to show that low frequency data are on the right side of the plot and higher frequencies are on the left.

The impedance Z(ω) is represented as a complex number:

$$Z(\omega) = \frac{\mathrm{E}}{\mathrm{I}} = Z_0 \times e^{j\varphi} = Z_0 \times (\cos(\varphi) + j \times \sin(\varphi)) \quad (3)$$

where:

E: potential;

I: current response;

Z_0: term of a magnitude;

ω: a radial frequency;

φ: a phase shift.

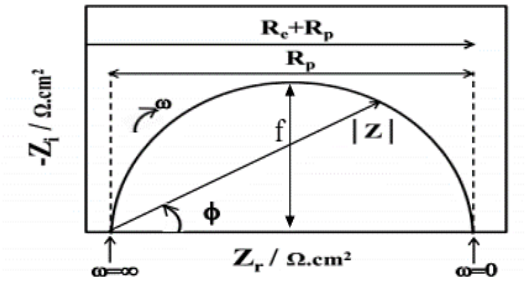

Fig. 2. Nyquist Plot with Impedance Vector

The spectra obtained by electrochemical impedance spectroscopy is shown in the Nyquist plane in Figure 3.

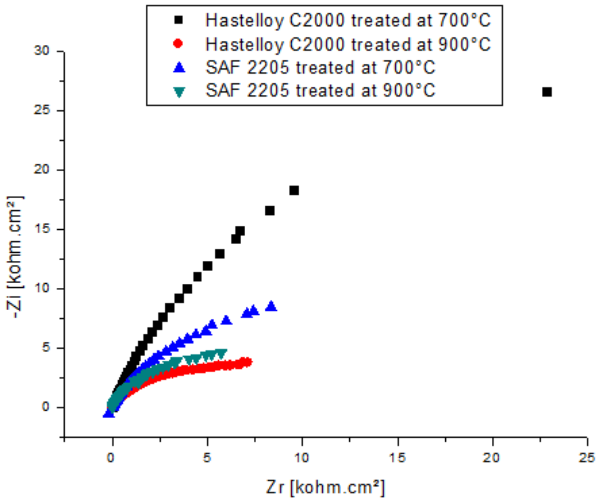

Fig. 3. Electrochemical Impedance Diagrams in the Nyquist plane for Hastelloy C2000 and SAF 2205 treated at 700 °C and 900 °C in 1 M H_3PO_4 at 100 mV/s

The Figure 3, shows that Nyquist diagrams have a large diameter capacitive loop characteristic of a passive layer. These diagrams also have the form of a semicircle, which means that the charge transfer is the main mechanism of the reaction at the interface/electrolyte level [29]. The analysis of the same Figure shows that among the electrochemical impedance spectroscopy curves of the two steels, the Hastelloy C2000 treated at 700 °C has a larger diameter of the semicircle, which means that this alloy has a better corrosion resistance in the phosphoric acid.

The simulation results of the equivalent electrical circuit is presented in Table 4.

Table 4. Dielectric parameters characterizing Hastelloy C2000 and SAF 2205 in 1 M H_3PO_4 after heat treatment at 700 °C and 900 °C

Steels	**Temperature**	**R_t**	**C_{dc}**
	°C	**Ω.cm²**	**µF/cm²**
Hastelloy C2000	700	72.39	19.36
	900	11.91	84.44
SAF 2205	700	25.60	62.16
	900	12.51	127.10

The rate of the resistance of transfer in percentage is calculated by the equation 4:

$$R_t\% = \frac{R_t(700°C) - R_t(900°C)}{R_t(700°C)} \times 100 \tag{4}$$

where R_t (700 °C) and R_t (900 °C) are the transfer resistance at the temperature treatment of 700 °C and 900 °C, respectively.

By analyzing the results presented in Table 4, it is noted that the transfer resistance (R_t) decreases with the rise in the temperature of the heat treatment of the same steel, with 83.55% for Hastelloy C2000 and 51,13% for SAF 2205. While for the capacity of the dual electric layer (C_{dc}), it increases with a difference that is almost the same for both steels and that is 65.08 µF/cm² for Hastelloy C2000 and 64.94 µF/cm² for SAF 2205.

This increase may also confirm the decrease in the thickness of the passive layer with the increase in the temperature of the treatment of the alloy. The comparison of these two parameters, between the Hastelloy C2000 and SAF 2205, shows that the transfer resistance (R_t) of the Hastelloy C2000 is greater than that of the SAF 2205 for a heat treatment at 700 °C, whereas it tends towards almost the same values for the heat treatment at 900 °C. While for the capacity of the double layer (C_{dc}) of the SAF 2205, it remains higher than that of the Hastelloy C2000. This shows the protective properties of the film formed on the Hastelloy C2000, which is in good agreement with the results founded previously.

3.1.3. Study of the pitting corrosion

The Figure 4 shows the various voltammograms recorded for the two steels SAF 2205 and Hastelloy C2000 for the study of the pitting corrosion resistance of these two alloys in the phosphoric acid.

The analysis of these voltammograms shows that the two steels present the same electrochemical behavior. For the stainless steels, such as Hastelloy C2000 and SAF 2205, the potential for pitting corrosion (E_{pitt}) occurs to the point where the current increases sharply due to stable pitting indicating sustained localized corrosion [30]. We present in the Table 5, the different values of E_{pitt} founded for Hastelloy C2000 and SAF 2205 steels, depending on the temperature of the heat treatment.

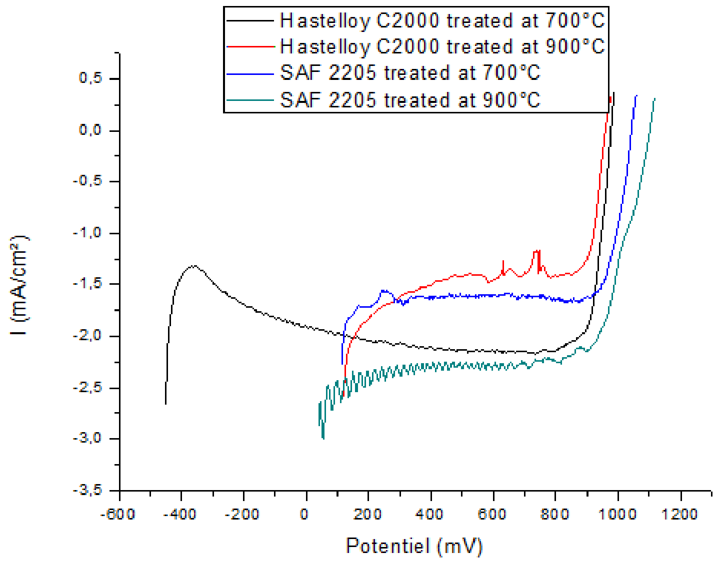

Fig. 4. Voltammograms of pitting corrosion for Hastelloy C2000 and SAF 2205 treated at 700 °C and 900 °C in 1 M H_3PO_4

Table 5. Pitting potential of Hastelloy C2000 and SAF 2205 in 1 M H_3PO_4 after heat treatment at 700 °C and 900 °C

Steels	Temperature	E_{pitt}
	°C	mV
Hastelloy C2000	700	924.50
	900	909.25
SAF 2205	700	875.50
	900	829.25

From the Figure 4, we noted that at more positives potentials, we have the presence of oscillations of the intensity of current. This finding was observed also by Pagetti [31], for a stainless steel in saturated solution KCl-NaCl and explained these oscillations as an expression of a balance between the local destruction of the protective film, which increases the intensity, and its reconstitution, which decreases it. Therefore, we can explain these oscillations encountered in our case by the variations of intensity. This phenomenon is more visualized for the SAF 2205 treated at 900 °C because of his high sensibility to the pitting corrosion.

From the Table 5, it can also be noted that the pitting potential of SAF 2205 is in the order of 829.25 mV at 900 °C and 875.5 mV at 700 °C. However, for the Hastelloy C2000, it is in the order of 909.25 mV at 900 °C and 924.5 mV at 700 °C. These pitting potential values for the both steels show that the pitting potential decreases with the elevation of the temperature of the heat treatment. Therefore, it can be concluded that an increase in the temperature of the heat treatment for the both steels reduces their resistances to pitting corrosion. It also noted that when the value of the potential is high, the steel resists more to this type of corrosion. The analysis of these results of the two steels also shows that the SAF 2205 is more disposed to this type of corrosion compared to the Hastelloy C2000. The mean results about comparison of electrochemical behavior of steels Hastelloy C2000 and SAF 2205 in 1 M H_3PO_4 are regrouped in Table 6.

Table 6. Corrosion parameters of Hastelloy C2000 and SAF 2205 in 1 M H_3PO_4

Steels	**Temperature**	E_{corr}	R_p	i_{corr}	R_t	C_{dc}	E_{pitt}
	°C	**mV *vs.* Ag/AgCl**	**Ω.cm^2**	**µA/cm^2**	**Ω.cm^2**	**µF/cm^2**	**mV**
Hastelloy C2000	700	-510.00	109.44	310.10	72.39	19.36	924.50
	900	-504.80	88.24	371.00	11.91	84.44	909.25
SAF 2205	700	-541.10	1380.00	21.06	25.60	62.16	875.50
	900	-531.10	328.35	84772.00	12.51	127.10	829.25

In the case of the SAF 2205, the two austenitic and ferritic phases can have different behaviors, and particularly different passivation layer thicknesses.

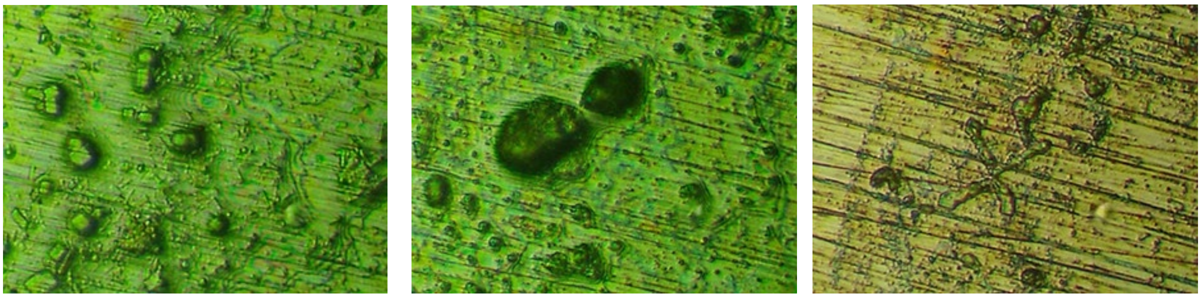

(a) **(b)** **(c)**

Fig. 5. Visualization by optical microscopy of structure of SAF 2205 heat treated after 20 days

It is noted that in very aggressive solution, such as phosphoric acid, there may also occur preferential dissolution of one of these phases and may lead to a weakening of the generalized corrosion resistance, which is directly linked to the intrinsic properties of the material to resist the mechanisms of corrosion encountered in this aggressive solution [32].

The previous microstructural and mechanical analysis also showed that for the SAF 2205, we have the formation of the χ phase. This phase has a severe influence on the resistance to pitting corrosion [33]. This precipitation is also accompanied by the presence of several intermetallic phases such as $M_{23}C_6$ carbide, sigma phase and secondary austenite (Figures 5 and 6). These phases damage the properties of steel due to the unequal distribution of alloy elements and their depletion in adjacent areas. It is also noted that the formation of sigma (Cr-rich phase) by the decomposition of the ferrite phase, for example, generally causes Cr depletion in the underlying regions, making them more susceptible to corrosion [34].

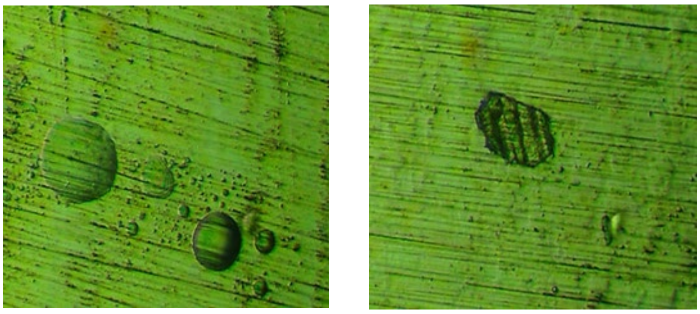

(a) (b)

Fig. 6. Visualization by optical microscopy of structure of SAF 2205 heat treated after 30 days

3.2. Influence of sulfate on the electrochemical behavior of Hastelloy C2000 and SAF 2205

The Figures 7 and 8 shows the anodic and cathodic polarization curves, successively, of the Hastelloy C2000 treated at 700 °C and SAF 2205 900 °C in 1 M H_3PO_4 in the presence of sulfate with a concentration ranging from 0.1 g/l to 0.7 g/l. The curves are obtained after 5 minutes of maintenance time of the working electrode with corrosion potential.

Different electrochemical parameters including corrosion potential (E_{corr}), corrosion current density (i_{corr}), and polarization resistance were obtained by extrapolating the polarization curve. All these parameters are listed in the Table 7 for each steel and according to the sulfate concentration.

The inhibition efficiency (IE_{Tafel}) values in percentage are calculated using the current densities (i_{corr}) values as expressed with the equation 5:

$$IE_{Tafel}\% = \frac{i_{corr}-i'_{corr}}{i_{corr}} \times 100 \qquad (5)$$

where i_{corr} and i'_{corr} uninhibited and inhibited corrosion current densities, respectively.

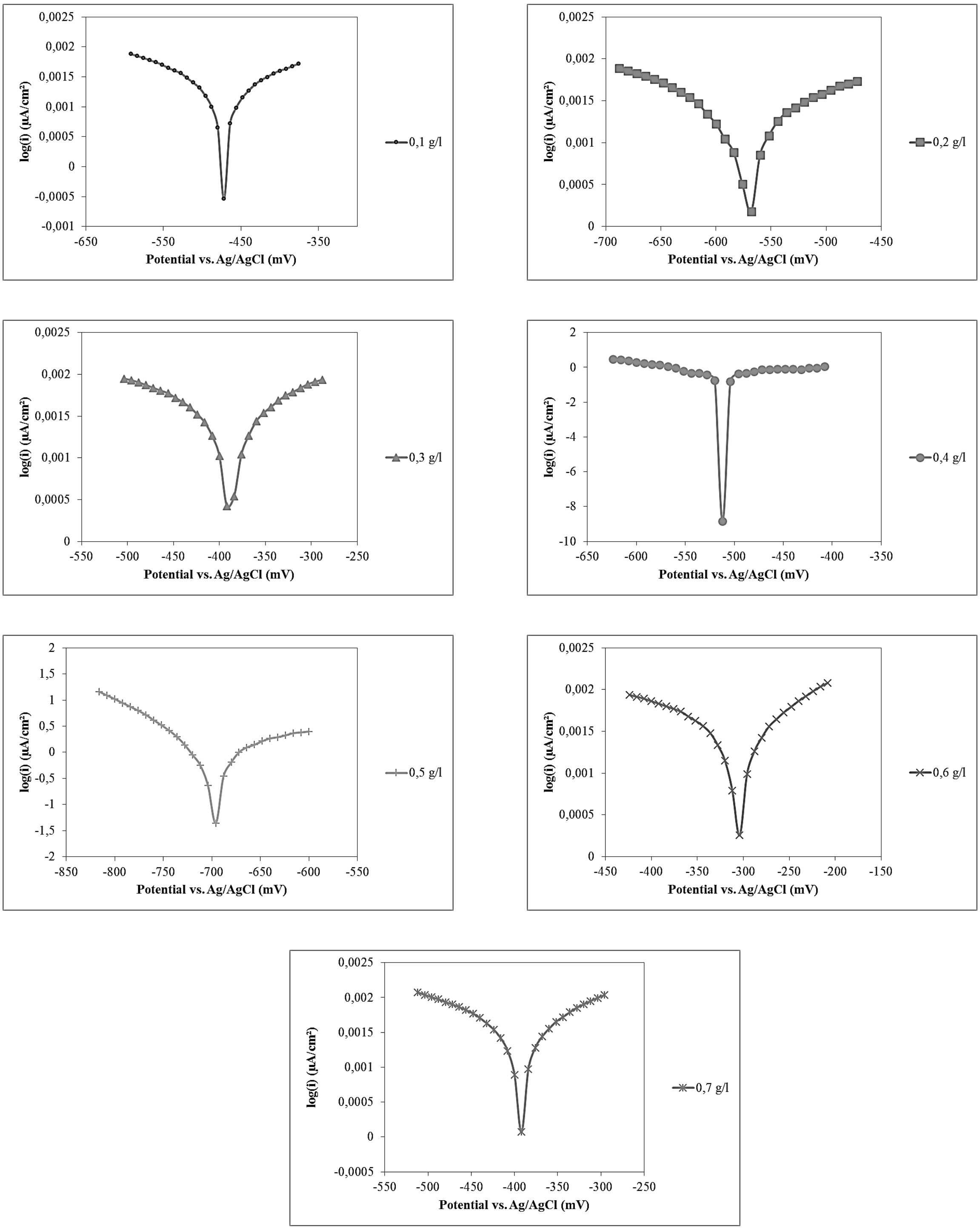

Fig. 7. Polarization curves for Hastelloy C2000 treated at 700 °C in 1 M H_3PO_4 solution containing Na_2SO_4 for various $[SO_4^{2-}]$

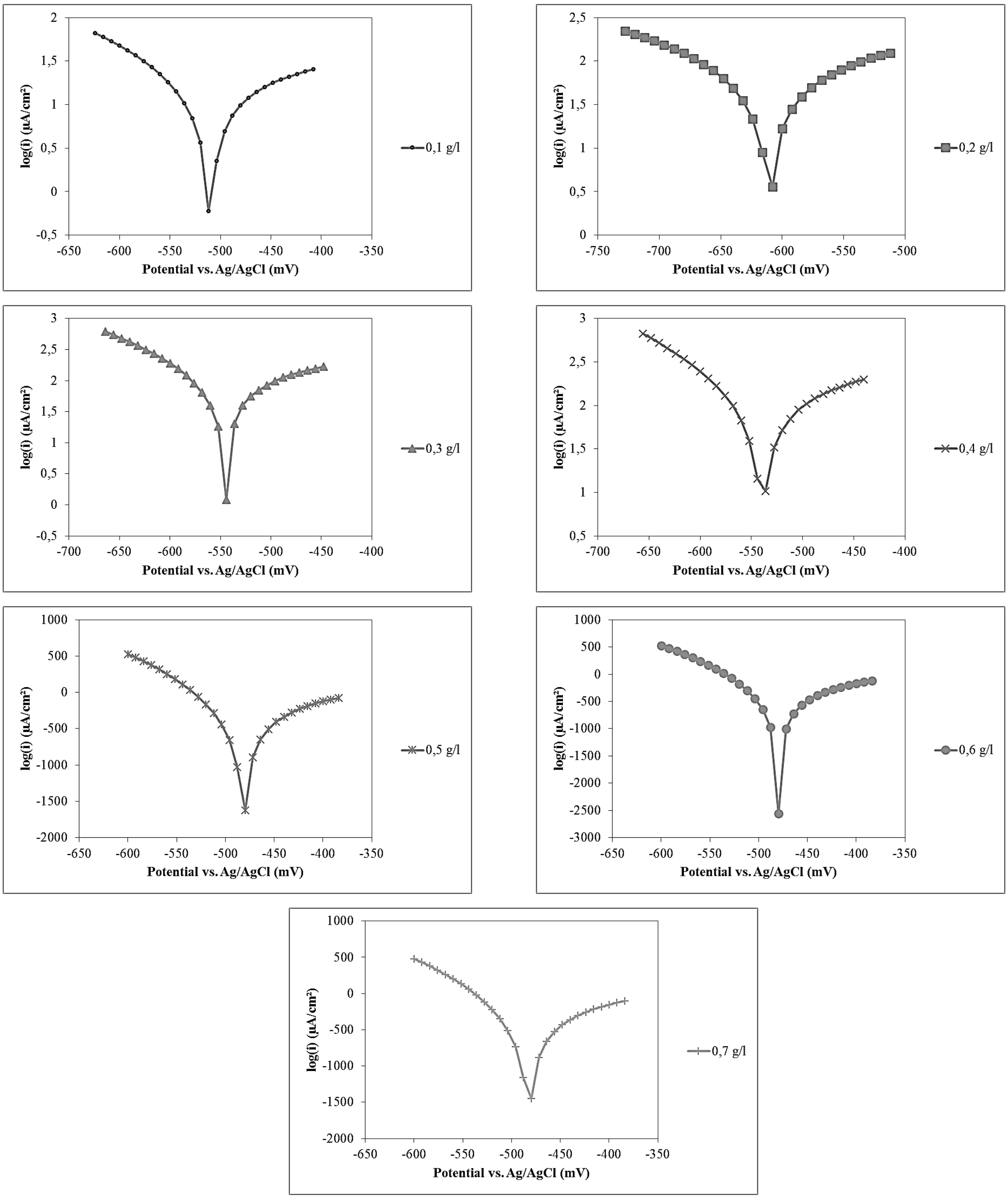

Fig. 8. Polarization curves for SAF 2205 treated at 900 °C in 1 M H_3PO_4 solution containing Na_2SO_4 for various $[SO_4^{2-}]$

The inhibition efficiency (IE_{Tafel} of R_p) values in percentage are calculated using the polarization resistance (R_p) values as expressed with the equation 6.

$$IE_{Tafel_{R_p}}\% = \frac{R'_p - R_p}{R'_p} \times 100 \qquad (6)$$

where R_p and R'_p uninhibited and inhibited corrosion polarization resistance, respectively.

Table 7. Corrosion parameters of Hastelloy C2000 and SAF 2205 as function of [SO_4^{2-}] in 1 M H_3PO_4 solution containing Na_2SO_4

Steels	**[SO_4^{2-}]**	**E_{corr}**	**R_p**	**i_{corr}**	**IE_{Tafel} of R_p**	**IE_{Tafel} of i_{corr}**
	g/l	**mV *vs.* Ag/AgCl**	**Ω.cm²**	**µA/cm²**	**%**	**%**
Hastelloy C2000	0,0	-510.00	1.09×10^{2}	3.10×10^{2}	0.00	0.00
	0,1	-471.40	1.74×10^{6}	1.92×10^{-2}	99.99	99.99
	0,2	-572.10	1.68×10^{6}	1.92×10^{-2}	99.99	99.99
	0,3	-387.00	1.18×10^{6}	2.84×10^{-2}	99.99	99.99
	0,4	-500.40	4.79×10^{4}	3.31×10^{-2}	99.77	99.89
	0,5	-693.20	2.98×10^{4}	9.18×10^{-2}	99.63	99.70
	0,6	-303.30	1.12×10^{6}	2.98×10^{-2}	99.99	99.99
	0,7	-391.60	9.61×10^{2}	3.31×10^{-2}	98.61	99.98
SAF 2205	0,0	-531.10	3.28×10^{2}	8.48×10^{4}	0.00	0.00
	0,1	-509.20	3.17×10^{3}	9.99×10^{1}	99.88	89.64
	0,2	-609.70	3.68×10^{3}	4.60×10^{1}	99.94	91.06
	0,3	-541.70	4.54×10^{2}	6.77×10^{4}	20.10	27.72
	0,4	-537.00	3.92×10^{2}	7.66×10^{4}	9.63	16.25
	0,5	-540.00	3.92×10^{2}	7.66×10^{4}	9.67	16.15
	0,6	-543.70	3.90×10^{2}	7.73×10^{4}	8.85	15.81
	0,7	-540.00	3.82×10^{2}	7.74×10^{4}	8.72	13.98

From the results obtained, we can note that for the Hastelloy C2000:

-The corrosion current intensity, for this alloy, decreases from its initial value which is 3.10×10^{2} (µA/cm²) to reach the value of 1.923×10^{-2} (µA/cm²) from the first addition of sulfate then it reaches its maximum for 0.5 g/l of [SO_4^{2-}];

-The polarization resistance increases considerably from its value of 1.09×10^{2} (Ω.cm²) to the value of 1.74×10^{6} (Ω.cm²) after the addition of sulfate to the phosphoric acid solution, then it begins to decrease with the increase of the concentration of the sulfate to the value of 9.61×10^{2} (Ω.cm²) for 0.7 g/l of [SO_4^{2-}]. This value remains much higher than that founded in previous results in phosphoric acid only.

For the SAF 2205, it is noted that:

-The corrosion current intensity decreases from its initial value of 8.48×10^{4} (µA/cm²) to 9.99×10^{1} (µA/cm²) from the first addition of the sulfate, then it continues to decrease to the minimum for 0.2 g/l of [SO_4^{2-}] and it stabilizes at 7.73×10^{4} (µA/cm²) for 0.7 g/l of [SO_4^{2-}];

-The polarization resistance increases from its initial value, which is 3.28×10^{2} (Ω.cm²), to reach the value of 3.17×10^{3} (Ω.cm²) with the addition of sulfate to the phosphoric acid solution. Then it reaches its maximum for 0.2 g/l of [SO_4^{2-}] and it continues to decrease until reaching the value of 3.82×10^2 ($\Omega.cm^2$) for 0.7 g/l of [SO_4^{2-}].

In order to understand the effect of the addition of sulfate, on the behavior of Hastelloy C2000 and SAF 2205 steels, we plotted the variation of the inhibitory efficiency of the corrosion current intensity as a function of the sulfate concentration. Figure 9 shows the variation of the inhibitory efficiency of the Hastelloy C2000 and SAF 2205 as a function of the sulfate concentration, [SO_4^{2-}], in the electrolytic solution.

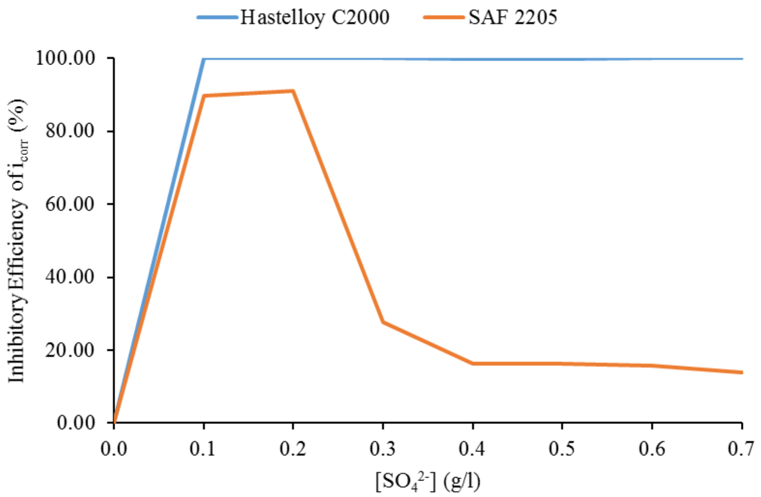

Fig. 9. Evolution of inhibitory efficiency of i_{corr} Hastelloy C2000 and SAF 2205 according to the variation of [SO_4^{2-}]

The comparison of the behavior of the Hastelloy C2000 (Figure 9), shows that a corrosion inhibition of 99,99% is observed with the addition of 0.1 g/l of [SO_4^{2-}]. This value remains almost constant with the increase in the sulfate concentration. This suggests, that the 0.1 g/l of [SO_4^{2-}] is the optimal value to achieve the better corrosion inhibition for Hastelloy C2000. These is also, confirmed by a high increase in polarization resistance, which is associated with a high corrosion prevention capacity [35].

The curve corresponding to the SAF 2205 in Figure 9 shows that for a concentration of 0.1 g/l of SO_4^{2-} the inhibitory efficiency is 89.64%. This efficiency reaches a maximum of 91.06% for 0.2 g/l of [SO_4^{2-}]. However, at higher sulfate concentrations, the inhibitory capacity of this ion decreased progressively to the minimum, as it is the example for 0.7 g/l of [SO_4^{2-}] where the inhibitory efficiency is 13.98%.

A study of the same SAF 2205 in the same sulfuric acid solution showed that higher corrosion rates were observed at higher concentrations. It has also been shown that this rise is due to the presence of the different intermetallic phases precipitating at high temperatures, especially the sigma phase, and the presence of the degraded areas with low chromium levels in the alloy structure [36]. These phases deteriorate and severely affect the corrosion of the alloy due to the unequal distribution of the alloy elements and their depletion in adjacent areas.

This is in line with the different results of the microstructural analysis carried out previously on Hastelloy C2000 and SAF 2205 [37].

Several studies [38,39] have also shown the significant influence of sulfate on the corrosion behavior of steels, which is reflected in its influence on nature, composition and thickness of the oxides layer formed. In addition, it has been shown, that for some steels that, when the sulfate concentration is high, the oxide layer tends to become weakly protective [38]. This reflects the behavior of SAF 2205 as a function of the increase in sulfate concentration.

However, a study of the stainless steel X2CrNi18-10 showed that the addition of sulfate to the electrolytic solution increases the passivity domain and displaces the pitting potential in the most noble direction, reflecting the beneficial role and inhibitory effect of SO_4^{2-}ions against chloride ions [40,41]. This was also confirmed by another study on the same alloy in a solution containing sulfuric acid in the presence of chloride ions [42]. These different studies clearly show the effect of adding sulfate in the electrolytic solution as a corrosion inhibitor. This is consistent with the study of the Hastelloy C2000 in a solution containing sulfate.

The comparison of the electrochemical behavior of the Hastelloy C2000 and SAF 2205, through their corrosion intensity, shows that the Hastelloy C2000 steel has a better corrosion resistance compared to the SAF 2205. This same result was visualized in a solution containing only phosphoric acid.

4. CONCLUSION

The electrochemical study of the two steels Hastelloy C2000 and SAF 2205, by analyzing the different parameters extrapolated from the Tafel curves in 1 M concentration phosphoric acid, showed that the corrosion resistance of SAF 2205 stainless steel is more affected than that of the Hastelloy C2000. This is shown by an increase of 19.63% in the corrosion intensity and a decrease of 19.37% in the polarization resistance of the Hastelloy C2000 and more important decrease of 76.21% for SAF 2205 steel with the increase in the temperature of the heat treatment. The electrochemical impedance spectroscopy shows that the rise in the temperature of the heat treatment of the same steel, causes a decrease in resistance, with a rate of 83.55% for the Hastelloy C2000 and of 51.13% for SAF 2205. The Analysis of the variation in corrosion current intensity versus potential also showed that the pitting potential of SAF 2205 stainless steel is greater than that of Hastelloy C2000, with a rate of 5.30% for the treatment at 700 °C and 8.79% for the treatment at 900 °C. The electrochemical behavior characterization tests of the two steels, in solution containing SO_4^{2-}, showed a significant difference in the corrosion sensitivity of Hastelloy C2000 to a solution containing only phosphoric acid, indicating the inhibitory effect of sulfate. The effect of the addition of sulfate was more significant with an efficiency of 99.99% for Hastelloy C2000. However, the same effect was more remarkable from the concentration of 0.2 g/l of [SO_4^{2-}], with an inhibition rate of 91.06% for SAF 2205. This rate decreases significantly for sulfate concentration greater than 0.2 g/l.

Conflict of interest

The author states no interest conflict for the submitted manuscript.

Acknowledgements

The author acknowledges the financial support of the National Center for Scientific and Technical Research (CNRST).

REFERENCES

[1] V. Aubin, Plasticité cyclique d'un acier inoxydable austéno-ferritique sous chargement biaxial non-proportionnel, Thèse, Université des Sciences et Technologies de Lille (2001) 16.

[2] V. B. Singh, and M. Ray, Int. J. Electrochem. Sci. 2 (2007) 329.

[3] Y. Lazhar, Thèse, Université Constantine (2013) 1.

[4] A. Bellaouchou, A. Guenbour, and A. Ben Bachir. Corrosion 49 (1993) 656.

[5] T. Poornima, J. Nayak, and A. Nityananda Shetty, Int. J. Electrochem. Sci. 5 (2010) 56.

[6] A. Guenbour, J. Faucheu, A. Ben Bachir, F. Dabosi, and N. Bui. Corrosion J. 23 (1988) 234.

[7] A. Bellaouchou, B. Kabkab, A. Guenbour, and A. Ben Bachir, Prog. Org. Coatings. 41 (2001) 127.

[8] L. Huabing, J. Zhouhua, F. Hao, S. Zhang, H. Peide, Z. Wei, L. Guoping, and F. Guangwei, Int. J. Electrochem. Sci. 10 (2015) 4832.

[9] A. C. Hart, British Corroion J. 6 (1971) 205.

[10] L. de Micheli, A. H. P. Andrade, C. A. Barbosa, and S. M. L. Agostinho, British Corrosion J. 34 (1999) 67.

[11] C. Escrivà-Cerdána, E. Blasco-Tamarit, D. M. García-García, J. García-Antón, R. Akid, and J. Walton, Electrochim. Acta 111 (2013) 552.

[12] C. Escrivà-Cerdán, E. Blasco-Tamarit, D. M. García-García, J. García-Antón, and A. Ben-Bachir, Int. J. Electrochem. Sci. 7 (2012) 5754.

[13] L. J. Yang, Y. Z. Xu, Y. Zhu, L. Liu, X. N. Wang, and Y. Huang, Int. J. Electrochem. Sci. 11 (2016) 6943.

[14] Y. L. Chou, Y. C. Wang, J. W. Yeh, and H. C. Shih, Corrosion Sci. 52 (2010) 3481.

[15] Z. P. Zhu, X. C. Jiao, X. Y. Tang, and H. W. Lu, Anti-Corrosion Method. 62 (2015) 322.

[16] S. Xiong, Z. Zhu, H. Zhang, and L. Jing. Corrosion 268 (2012) 015001.

[17] J. O. Nilsson, J. Mater. Sci. Technol. 8 (1992) 685.

[18] K. M. Lee, H. S. Cho, and D. C. Choi, J. Alloy. Compound. 285 (1999) 156.

[19] P. A. Schweitzer, Fundamentals of Metallic Corrosion: Atmospheric and Media Corrosion of Metals 9780849382437 (2006) 200.

[20] R. Iuliano, Master. Eng. (2014) 12.
[21] Y. S. Zhang, X. M. Zhu, and S. H. Zhong, Corrosion Sci. 46 (2004) 853.
[22] C. O. A. Olsson, and D. Landolt, Electrochim. Acta 48 (2003) 1093.
[23] M. Reffass, R. Sabot, M. Jeannin, C. Berziou, and P. Refait, Electrochim. Acta 54 (2009) 4389.
[24] L. Huabing, S. Wang, B. Fang, S. Zhang, and W. Liu, Int. J. Electrochem. Sci. 10 (2015) 4832.
[25] R. Sánchez-Tovar, M. T. Montañés, J. García-Antón, and A. Guenbour, Int. J. Electrochem. Sci. 6 (2011) 3656.
[26] S. Bakour, Int. J. Electrochem. Sci. 7 (2012) 10530.
[27] J. Pan, C. Leygraf, R. F. A. Jargelius-Pettersson, and J. Lindén, Oxid/ Metals. 50 (1998) 431.
[28] M. J. Carmezim, A. M. Simões, M. F. Montemor, and M. Belo, Corrosion Sci. 47 (2005) 581.
[29] L. Larabi, Y. Harek, M. Traisnel, and A. Mansri, J. Appl. Electrochem. 34 (2004) 833.
[30] D. Tromans, and A. Sato, Corrosion. 57 (2001) 126.
[31] G. Daufin, and J. Talbot, INRA Editions. 51 (1971) 661.
[32] B. Belkessa, Université Saad Dahleb de Blida. (2005) 12.
[33] N. Ouali, Université Saad Dahlab de Blida. (2012) 35.
[34] A. Gregori, and J. O. Nilson, Metallurg. Transac. 33A (2002) 1009.
[35] P. Gu, B. Arsenault, J. J. Beaudoin, J. G. Legoux, B. Harvey, and J. Fournier, Cement and Concrete Res. 28 (1998) 321.
[36] K. Ravindranath, and S. N. Malhotra, Corrosion Sci. 37 (1995) 121.
[37] A. Amri, O. Benlenda, F. Sabir, L. Zerrouk, A. Ibnlfassi, and E. Saad, J. Sci. Arts. 4 (2016) 363.
[38] S. M. Abd El Haleem, S. Abd El Wanees, E. E. Abd El Aal, and A. Diab, Corrosion Sci. 52 (2010) 292.
[39] P. Ghods, O. B. Isgor, G. McRae, and T. Miller, Cement and Concrete Composite. 31 (2009) 2.
[40] R. M. Carrranza, and M. G. Alvarez, Corrosion Sci. 38 (1996) 909.
[41] H. P. Leckie, and H. H. Uhlig, J. Electrochem. Soc. 113 (1966) 1262.
[42] R. T. Loto, J. Mater. Environ. Sci. 4 (2013) 448.